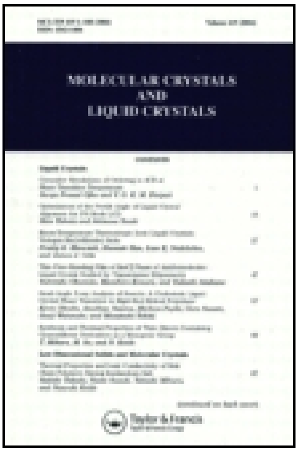

Molecular Crystals and Liquid Crystals
Publication details, including instructions for authors and subscription information:
http://www.tandfonline.com/loi/gmcl20

Investigating the Stabilisation Effect of Carboxylic vs. Hydroxyl Groups on Fe_3O_4 and Fe_3O_4@Au Nanoparticles

Hendriëtte van der Walt [a], Lesley Chown [a], Ndabenhle Sosibo [a] & Robert Tshikhudo [a]
[a] NIC, Mintek, Private Bag X3015, Randburg, Johannesburg, South Africa

To cite this article: Hendriëtte van der Walt, Lesley Chown, Ndabenhle Sosibo & Robert Tshikhudo (2012): Investigating the Stabilisation Effect of Carboxylic vs. Hydroxyl Groups on Fe_3O_4 and Fe_3O_4@Au Nanoparticles, Molecular Crystals and Liquid Crystals, 555:1, 1-6

To link to this article: http://dx.doi.org/10.1080/15421406.2012.634351

Mol. Cryst. Liq. Cryst., Vol. 555: pp. 1–6, 2012
Copyright © Taylor & Francis Group, LLC
ISSN: 1542-1406 print/1563-5287 online
DOI: 10.1080/15421406.2012.634351

Investigating the Stabilisation Effect of Carboxylic vs. Hydroxyl Groups on Fe_3O_4 and Fe_3O_4@Au Nanoparticles

HENDRIËTTE VAN DER WALT,* LESLEY CHOWN,
NDABENHLE SOSIBO, AND ROBERT TSHIKHUDO

NIC, Mintek, Private Bag X3015, Randburg, Johannesburg, South Africa

The high-temperature solution phase reaction of iron(III) acetylacetonate, Fe(acac)$_3$ and 1,2-hexadecanediol was used to synthesise iron oxide and gold-coated iron oxide nanoparticles. Different surface functionalities, such as sebacic acid (SA) and 1, 10–Decanediol (DD), were introduced on the surface of the particles to investigate the stabilising effect of carboxylic groups (SA) in comparison to the hydroxyl groups (DD). Nanoparticle thermal stability, composition, state of aggregation, size and morphology were investigated and the results from techniques such as Fourier Transform-Infra Red spectroscopy (FT-IR), Ultraviolet visible spectroscopy (UV-vis), Transmission Electron Microscopy (TEM) and thermal analysis are discussed.

Keywords 1,10-Decanediol; Fe_3O_4; Fe_3O_4@Au; magnetite; nanoparticles; sebacic acid

Introduction

A magnetic fluid is a stable colloidal suspension of magnetic nanoparticles dispersed in a carrier liquid [1]. Magnetic nanoparticles show very interesting electrical, optical, magnetic, and biochemical properties, illustrating novel applications in biomedical imaging, clinical diagnosis, biosensors and drug delivery systems. The potential of these nanofluids is disclosed by surface modification through the interaction of the functional groups on the surfactant molecules [2]. Iron oxide nanoparticles are widely studied materials, as they occur naturally, are rapidly synthesised artificially, have attractive chemical and magnetic properties and applications in *in* vivo magnetic imaging [3]. Gold coating of magnetic nanoparticles is a very attractive technique, as the magnetic nanoparticles can be both stabilised more effectively in corrosive biological conditions and easily functionalised through well-developed Au-S chemistry. The coating also provides the magnetic nanoparticles with plasmodic properties, making them extremely useful for magnetic, optical and biological applications [4]. The high-temperature solution phase reaction of iron(III) acetylacetonate, Fe(acac)$_3$ and 1,2-hexadecanediol was used to synthesise iron oxide and gold-coated iron oxide nanoparticles. Different surface functionalities, such as sebacic acid (SA) and 1, 10–Decanediol (DD), were introduced on the surface of the particles to investigate the

---

*Address correspondence to H. van der Walt, NIC, Mintek, Private Bag X3015, Randburg, Johannesburg, South Africa. Tel: +27 (0)11 709 4757; Fax: +27 (0)11 709 4800; E-mail: hendriettep@mintek.co.za stabilising effect of carboxylic groups (SA) in comparison to the hydroxyl groups (DD). Nanoparticle thermal stability, composition, state of aggregation, size and morphology were investigated and the results from techniques such as Fourier Transform-Infra Red spectroscopy (FT-IR), Ultraviolet visible spectroscopy (UV-vis), Transmission Electron Microscopy (TEM) and thermal analysis are discussed.

Experimental

The Fe_3O_4 and Fe_3O_4@Au nanoparticles were prepared as previously reported [11,12], with SA and DD as the surfactants. The Fe_3O_4 nanoparticles were synthesised using SA (0.606 g; 3 mmol) or DD (0.522 g; 3 mmol), whereas the Fe_3O_4@Au nanoparticles were synthesised using SA or DD stabilised Fe_3O_4 nanoparticles (1 ml) along with SA (0.030 g; 0.15 mmol) or DD (0.026 g; 0.15 mmol).

Results

The FT-IR spectra (Fig. 1(a)) confirmed the basic structure of the SA and DD surfactants on the Fe_3O_4 nanoparticles, showing characteristic CH_2 peaks noted. The spectra shows the transformation of the initial carboxylic acids (COOH – 1690 cm^{-1}) of the SA to carboxyl ions (COO^- – 1568 cm^{-1} and 1446 cm^{-1}) and the transformation of the initial hydroxyl groups (OH – 3401 cm^{-1} and 3338 cm^{-1}) of DD to oxygen ions (O^- - broad 3290 cm^{-1}).

Although the UV-vis spectra (Fig. 1(b)) showed the Fe_3O_4 nanoparticles with no absorbance [13,14], absorbance was seen for the particles coated with gold. The absorbance for the SA stabilised Fe_3O_4@Au nanoparticles was 512 nm, while the DD stabilised Fe_3O_4@Au nanoparticles showed absorbance at 518 nm. This illustrated that although the Au shell thickness was the same for both of the nanoparticle samples (Fig. 2), the Au shell surface area of the SA and DD stabilised Fe_3O_4@Au nanoparticles differed, because of the difference in size of the nanoparticles Fe_3O_4 core. This thus allowed the sizes of the nanoparticles to be quantified. This showed that the absorbance difference could be linked to the size difference between the two nanoparticle species, results also confirmed by the TEM images (Fig. 2). The complete coating of the Fe_3O_4 nanoparticles with Au was confirmed by not only the sharpness of the single absorbance peaks, but also by etching studies conducted on the samples using concentrated hydrochloric acid (HCl). Concentrated HCl dissolves the basic Fe_3O_4 nanoparticles, but leaves the Au shell unaffected. Thus, if the Au coated Fe_3O_4 nanoparticles had an incomplete Au shell, the acid would eat away / dissolve the Fe_3O_4 core, resulting in a collapse of the coated particles. Results showed no change in the TEM images and thus no nanoparticle etching or collapse, confirming the complete coating of the Fe_3O_4 nanoparticle with Au.

The structural images for the Fe_3O_4 and Fe_3O_4@Au nanoparticles are shown in Fig. 2. The surfactants are identical except for the carboxylic (SA) and hydroxyl (DD) functional groups and so it was predicted that the nanoparticles would be of similar size. The TEM images indicated a ± 3.73 nm variation in size (SA 2.00 ± 0.41 nm; DD 5.73 ± 1.08 nm) however, most probably due to the greater stability provided by the carboxylic acid of the SA in comparison to the hydroxyl groups of the DD.

A large number of artefacts was seen for the DD stabilised nanoparticles, although both the SA and DD stabilised Fe_3O_4@Au nanoparticles showed little aggregation. It is believed that the artefact particles are uncoated Fe_3O_4 nanoparticles bonded to and trapped in between the gold coated nanoparticles. This is supported by the size of the artefacts (5.33 ± 1.50 nm) and the fact that they were not removed during the vigorous cleaning

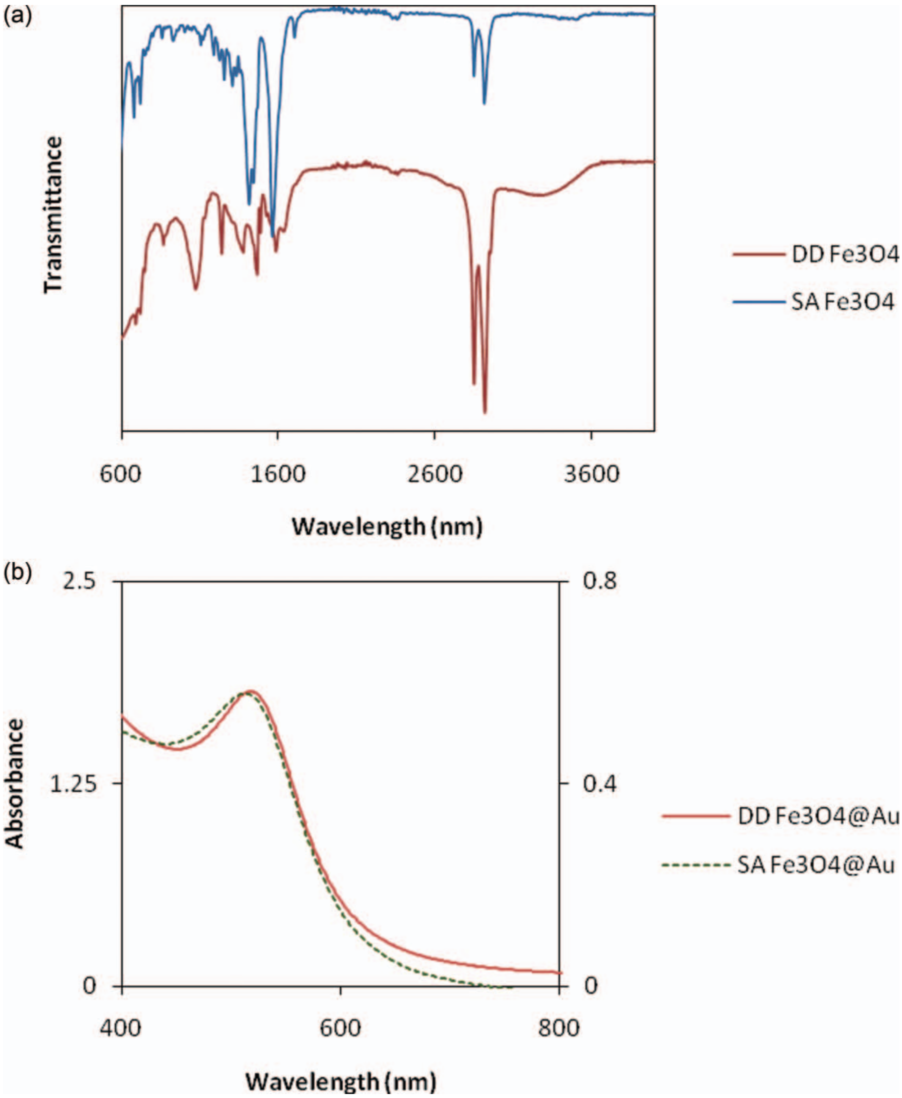

Figure 1. (a) FT-IR spectra of the DD and SA stabilised Fe_3O_4 nanoparticles; (b) UV-absorbance for the DD and SA stabilised Fe_3O_4 and Fe_3O_4@Au nanoparticles.

procedure. The DD stabilised Fe_3O_4@Au nanoparticles (8.60 ± 1.49 nm) were larger that the SA stabilised Fe_3O_4@Au nanoparticles (5.02 ± 1.00 nm). This, along with the artefacts, supports the theory that the carboxylic acids stabilise the iron oxide nanoparticles to a greater extent, giving better quality particles with narrower size distribution. The etching studies explained above showed dissolution of the artefact particles observed in the DD stabilised Fe_3O_4@Au nanoparticles. This provided additional confirmation that the artefacts were trapped Fe_3O_4 nanoparticles.

The stability of the nanoparticles was further investigated with the use of DSC and TGA. The results for the SA and DD stabilised nanoparticles are shown in Fig. 3. Figure 3(a) shows 2-stage mass changes for the DD stabilised Fe_3O_4 and Fe_3O_4@Au nanoparticles.

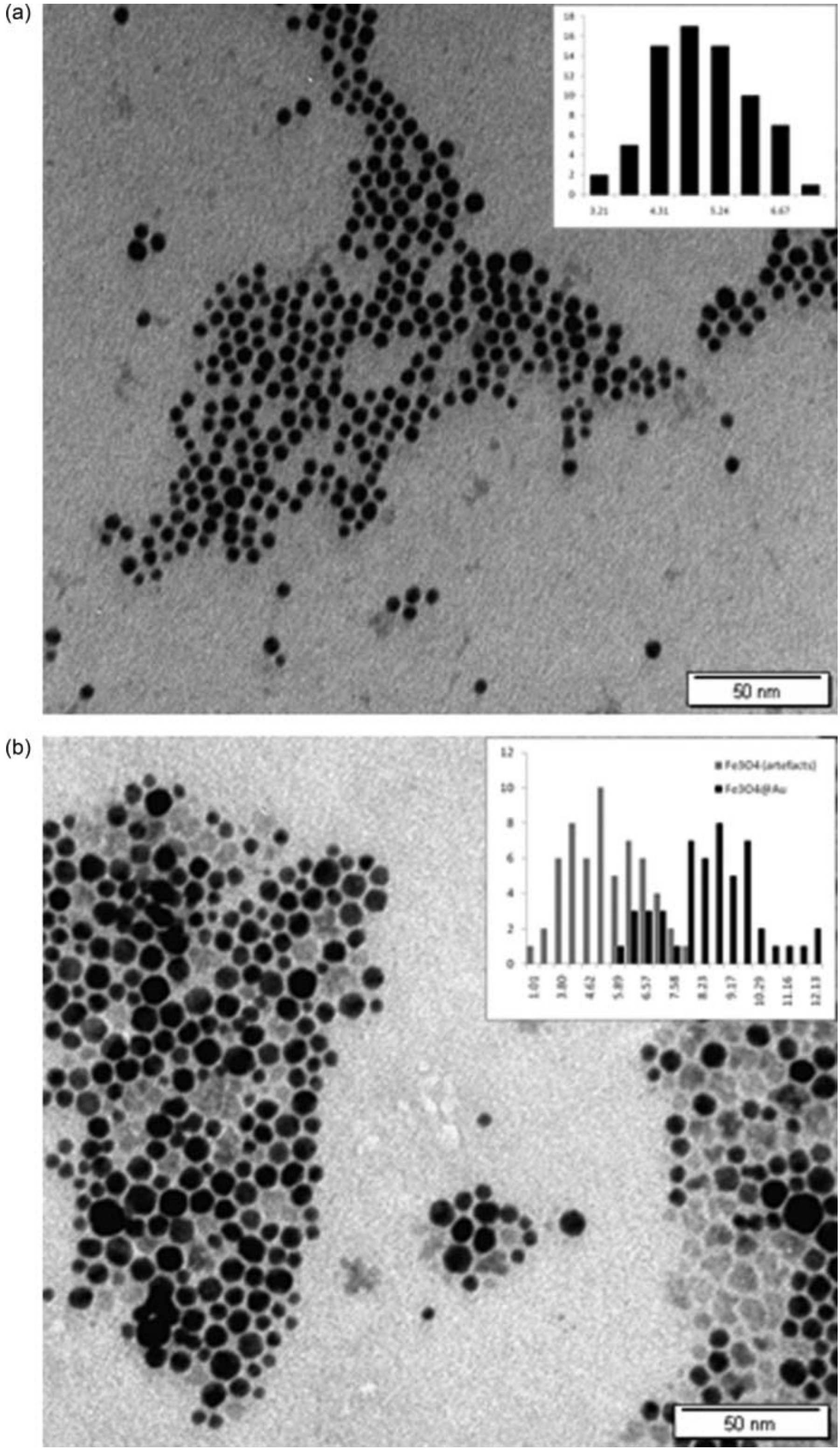

Figure 2. TEM images depicting the (a) SA stabilised Fe_3O_4@Au nanoparticles and (b) DD stabilised Fe_3O_4@Au nanoparticles. Scale bars indicate 50 nm.

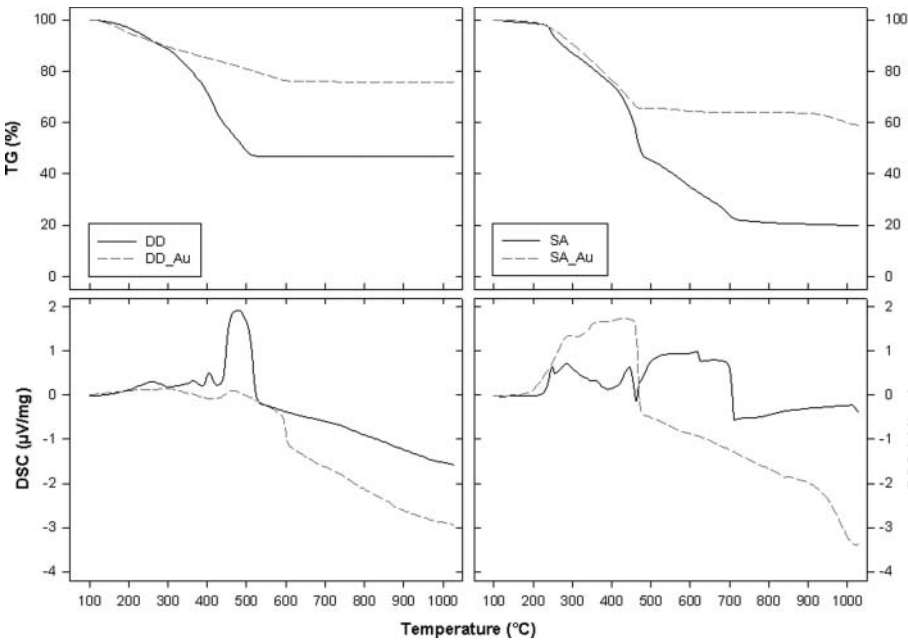

Figure 3. Thermal analysis of the DD stabilised Fe_3O_4 and Fe_3O_4@Au nanoparticles TGA (a) and DSC (b) and SA stabilised Fe_3O_4 and Fe_3O_4@Au nanoparticles TGA (c) and DSC (d).

The DD Fe_3O_4@Au nanoparticles showed no change in mass above 555°C, while the Fe_3O_4 nanoparticles showed negligible mass loss above 610°C.

The DSC response (Fig. 3(b)) shows four exothermic reactions associated with the mass loss steps for the DD stabilised Fe_3O_4 nanoparticles. There are two broad exothermic reaction peaks over the mass loss range for the DD stabilised Fe_3O_4@Au nanoparticles. The end of the exothermic reactions is associated with the end of mass loss.

Figure 3(c) shows 4-stage and 2-stage mass changes for the SA stabilised Fe_3O_4 and Fe_3O_4@Au nanoparticles respectively. The SA Fe_3O_4@Au nanoparticles displayed negligible mass loss from 480-875°C, followed by mass loss from 875°C to 1030°C. For the Fe_3O_4 nanoparticles, mass loss was significant from 200°C to 730°C.

The DSC curves in Fig. 3(d) show similar onset and end temperatures (~220°C and 470°C) of complex exothermic reactions for both SA stabilised Fe_3O_4 and Fe_3O_4@Au. SA stabilised Fe_3O_4 has an additional broad exothermic peak from 470°C to 705°C, which is associated with a large loss in mass (23%).

Although it is clearly seen that the Au shell improves the overall stability of the nanoparticles, it cannot overcome the poor stabilising ability of the DD hydroxyl groups. The 25% larger mass loss seen in Fig. 3(a) for the DD stabilised Fe_3O_4 in comparison to the SA Fe_3O_4 nanoparticles in Fig. 3(c), indicates the need for a larger particle core size (thus aggregating to lower the total energy) and more ligands to stabilise it. This leads to conclude that the carboxylic moieties of the SA stabilise the Fe_3O_4 nanoparticle to a larger extent.

Conclusion

In conclusion, the SA and DD stabilised Fe_3O_4 and Fe_3O_4@Au nanoparticles were successfully synthesised. FT-IR confirmed the presence of the DD and SA surfactants on the nanoparticles, while the gold coating of the nanoparticles was confirmed by UV-vis spectrometry, with variation in absorbance indicative of a change in volume of the Au shell. The sizes of the nanoparticles were determined by TEM. The ± 3.73 nm smaller SA Fe_3O_4 nanoparticles indicate the enhanced stabilising effect of the SA in relation to the DD. The DD stabilised Fe_3O_4@Au nanoparticles show a large amount of artefacts, believed to be uncoated Fe_3O_4 nanoparticles bonded to and trapped in between the gold coated nanoparticles for additional stability. Thermal analysis indicated that the Fe_3O_4@Au nanoparticles showed greater stability, with ± 40% less mass loss than the nanoparticles without gold and it confirmed the stability of the SA Fe_3O_4 nanoparticles above the DD Fe_3O_4 nanoparticles with a 25% reduction in core size from the SA to DD stabilised nanoparticles. All the characterisation preformed points to the carboxylic acids of the SA stabilising the nanoparticles to a greater extent when compared with the hydroxyl groups of the DD.

Acknowledgment

We would like to thank The University of KwaZulu-Natal for the TEM analysis. We would also like to thank Mintek for permission to publish the paper and for financial support.

References

[1] Shen, L., Laibinis, P. E., & Hatton, T. A. (1999). *Langmuir*, *15*, 447.

[2] Lyon, J. L., Fleming, D. A., Stone, M. B., Schiffer, P., & Williams, M. E. (2004). *Nano Lett.*, *4*, 719.

[3] Liu, H. L., Sonn, C. H., Wu, J. H., Lee, K-M., & Kim, Y. K. (2008). *Biomaterials*, *29*, 4003.

[4] Park, H-Y., Schadt, M. J., Wang, L., Lim, I. S., Njoki, P. N., Kim, S. H., Jang, M-Y., Luo, J., & Zhong, C-J. (2007). *Langmuir*, *23*, 9050.

[5] Chikate, R. C., Jun, K-W., & Rode, C. V. (2008). *Polyhedron.*, *27*, 933.

[6] Cabot, A., Puntes, V. F., Shevchenko, E., Yin, Y., Balcells, L., Marcus, M. A., Hughes, S. M., & Alivisatos, A. P. (2007). *J. Am. Chem. Soc.*, *129*, 10358.

[7] Koh, I., Wang, X., Varughese, B., Isaacs, L., Erhman, S.H., & English, D.S. (2006). *J. Phys. Chem. B.*, *110*, 1553.

[8] Bronstein, L. M., Huang, X., Retrum, J., Schmucker, A., Pink, M., Stein, B. D., & Dragnea, B. (2007). *Chem. Mater.*, *19*, 3624.

[9] Xu, Z., Hou, Y., & Sun, S. (2007). *J. Am. Chem. Soc.*, *129*, 8698.

[10] Cho, S-J., Idrobo, J-C., Olamit, J., Liu, K., Browning, N. D., & Kauzlarich, S. M. (2005). *Chem. Mater.*, *17*, 3181.

[11] Gangopadhyay, P., Gallet, S., Franz, E., Persoons, A., & Verbiest, T. (2005). *IEEE Trans. Magnet.*, *41*, 4194.

[12] Wang, W., Luo, L., Fan, Q., Suzuki, M., Suzuki, I. S., Engelhard, M. H., Lin, Y., Kim, N., Wang, J. Q., & Zhong, C-J. (2005). *J. Phys. Chem. B.*, *46*, 21593.

[13] Huang, J-H., Parab, H. J., Liu, R-S., Lai, T-C., Hsiao, M., Chen, C-H., Sheu, H-S., Chen, J-M., Tsai, D-P., & Hwu, Y-K. (2008). *J. Phys. Chem. C.*, *112*, 15684.

[14] Sun, S., Zeng, H., Robinson, D. B., Raoux, S., Rice, P. M., Wang, S. X., & Li, G. (2004). *J. Am. Chem. Soc.*, *126*, 273.